Proceedings of the ASME 2016 Fluids Engineering Division Summer Meeting
FEDSM16
July 10-14, 2016, Washington, DC, USA

PIV STUDY OF MILDLY CONTROLLED FLOW OVER A WING MODEL USING A SYNTHETIC JET ARRAY

Pramod B. Salunkhe
Associate Professor
Department of Mechanical Engineering
Pad. Dr. D.Y. Patil Institute of Engineering,
Management & Research
Pune, Maharashtra, India

Hui Tang
Assistant Professor
Department of Mechanical Engineering
The Hong Kong Polytechnic University
Kowloon, Hong Kong, China

Yanhua Wu
Assistant Professor
School of Mechanical &Aerospace Engineering
Nanyang Technological University
50 Nanyang Avenue, Singapore

ABSTRACT

This work describes the use of a synthetic jet (SJ) array for mild control of flow separation over a straight wing model. Experiments were performed in a subsonic wind tunnel to show improvement of the wing aerodynamic performance. A tomographic particle image velocimetry system was used to measure and analyze the three-dimensional flow-field with and without the SJ actuation. It was observed that, although the SJ array is relatively weak, it can still made impacts on the separated flow. After the SJ actuation, the large-scale vortex structures in the shear layer were broken into small discrete structures and the near-wall flow was substantially improved. Subsequently, Proper Orthogonal Decomposition (POD) analysis was also conducted and the effectiveness of the present SJ array was further discussed.

INTRODUCTION

Synthetic jet (SJ), also known as a zero-net-mass-flux jet, provides a novel means of flow control due to its ability of injecting non-zero momentum into external flow with zero net mass flux [1-6]. A typical SJ actuator consists of a cavity with an oscillatory diaphragm on its bottom side and an orifice on the opposite. The diaphragm's periodic downward and upward motion generates a succession of vortex rings/pairs that propagate away from the orifice/slot, synthesizing a SJ. Since emerging, its capability in flow separation control has been well demonstrated in many lab experiments [7-10]. However, different from all existing SJ-based flow separation control done by other researchers where strong enough SJs (momentum coefficient greater than 10^{-4}) were used, the present study aims to unveil flow details of mildly controlled separated flow over a straight-wing model using a SJ array that operates with a relatively small momentum coefficient (4.2×10^{-5}). In addition to the hot-wire and force measurement results released in our previous work [6], a key portion of the flow over the wing's suction surface with and without the SJ control is measured using a three-dimensional tomographic particle image velocimetry (Tomo-PIV) system. Both time-averaged and phase-locked PIV results are presented and analyzed to show the effect of this control. The proper orthogonal decomposition (POD) analysis is also applied to reveal meaningful difference between the flow fields with and without the SJ control.

EXPERIMENTAL SETUP

Experiments are carried out on a low-speed straight-wing model, LS(1)-0421MOD, in a subsonic wind tunnel of test section size, 0.8 m (W) × 0.8 m (H) × 2 m (L). The wing model has the chord length of 180 mm and span of 255 mm. The SJ actuator comprises of four 20 mm diameter piezoelectric diaphragms attached on its four sidewalls, as shown in Fig. 1(a). Multiple such actuators are arrayed and incorporated inside the wing model. An orifice of the SJ actuator comprises of five 1-mm-diameter holes in a row on the wing model, with a center-to-center distance of 2 mm between the successive holes. An array of such ten SJ actuators is located at 23% of the chord. The SJ array is excited in phase using two power amplifiers, which are interfaced with a function generator to generate sinusoidal waveforms at various voltages and frequencies.

In the present study, a three-dimensional Tomo-PIV system is used to capture the flow-field, as shown in Fig. 1(b). A pair of high energy Nd:YAG laser is used to illuminate the flow over the wing model suction surface to produce a laser volume sheet of 68 mm (x) × 56 mm (y) × 7 mm (z). The laser volume sheet is aligned in such a way that it covers a half of the second SJ actuator in the array, with its left edge right across the center

of the third hole and its right edge falling between two neighboring actuators.

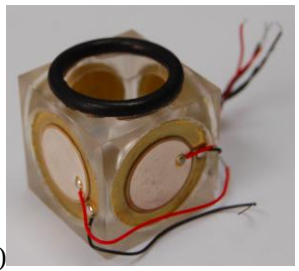

(a)

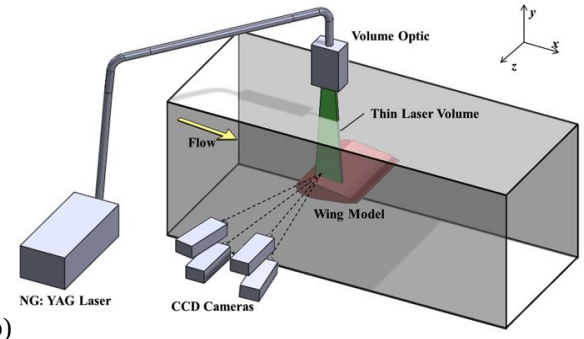

(b)

Fig. 1 (a) A SJ actuator (b) Setup of Tomo-PIV measurements

All PIV measurements are carried out at a constant wind speed U_∞ = 10 m/s and a fixed angle of attack 19°. The corresponding chord Reynolds number is 1.2×10^5. The SJ array is operated at 200 V excitation voltage and 400 Hz frequency that is close to the actuator's Helmholtz frequency. Under this condition, the corresponding momentum coefficient is about 4.2×10^{-5}. The phase-locked PIV measurements are carried out at eight different phase angles, where the phase angle of the SJ array is defined based on the output signal from the function generator, with the crest at phase angle 90° and the trough at 270°. At each phase angle, 200 pairs of seeding particle images are recorded by each of the four CCD cameras.

The uncertainty in PIV measurement is found to be 0.1 voxel for both streamwise and normal velocity components and 0.15 voxel for spanwise velocity component.

RESULTS AND DISCUSSION

Figure 2 shows 3D vortex structures colored by streamwise velocity, with velocity vectors and contours illustrated in the background, for the time-averaged baseline case, time-averaged SJ actuation case and eight phase-locked SJ actuation cases. These vortex structures are identified using iso-surfaces of local swirling strength. Most of the vortex structures fall within the shear layer that splits the flow field into two distinct flow regions, i.e., a free-stream flow region ($u/U_\infty > 1.5$) and a near-wall retarding flow region ($u/U_\infty < 0.5$). The baseline case shows substantial congestion of large-size vortex structures in the shear layer. After switching on the SJ array, significant alteration in the flow field can be observed as evident in the time-averaged and eight phase-averaged vortex/velocity fields.

Furthermore, the eight phase-averaged flow fields reveal that the interaction between the SJs and the boundary layer flow results in the formation of near-wall spanwise vortices. The formation and propagation of a specific vortex is marked with an arrow in Fig. 2 subplots. Instead of being directly generated from the SJs, this near-wall vortex is induced by the SJ and shed from the separated shear layer. During its downstream travelling, this vortex grows its size and strength successively up to the phase angle of 180° when the SJ operates near its maximum blowing. The largest improvement in the flow field also occurs at 180° as evident from the significant reduction in large-scale vortex structures in the shear layer zone as well as the substantial increase in the velocity of the near-wall flow as depicted by enlarged region of green and yellow color contours.

Although the SJ array helps re-energize the new-wall flow, this energy addition is not very significant due to the current moderate jet momentum coefficient. This mild energy addition does not completely eliminate the flow separation but positively alters the local flow field and reduces the intensity of the flow separation. This statement is supported by the observation of instantaneous flow fields. The instantaneous PIV images presented in Fig. 3 show that the flow over the wing suction surface is "flapping", which is sometimes attached and sometimes separated. The flow separation is observed even after switching on the SJ array. The statistics reveal that without the SJ actuation the attached flow and separated flow appeared almost evenly, whereas the attached flow became dominant with the SJ actuation.

The POD analysis further supports the above statement. It helps unravel dominant flow structures in an unsteady flow-field. In a typical POD method, eigen values, eigen vectors and finally eigen functions are determined from a given number of snapshots. The reconstructed flow-field can be given as

$$u^*(x,y,t) = \bar{u}(x,y) + \sum_{i=1}^{N} q_i(t)\Phi_i(x,y)$$

where u^* is the reconstructed velocity field, $\bar{u}$ the mean velocity, Φ_i the ith POD mode or eigen function, q_i the temporal coefficient corresponding to the ith POD mode, and N the number of POD modes used in the reconstruction. The POD modes can be computed by

$$\Phi_i(x,y) = \frac{1}{\sqrt{\lambda_i M}} \sum_{j=1}^{M} u'(x,y,t_j) q_i(t_j)$$

where λ_i are the eigen values, u' the instantaneous fluctuating

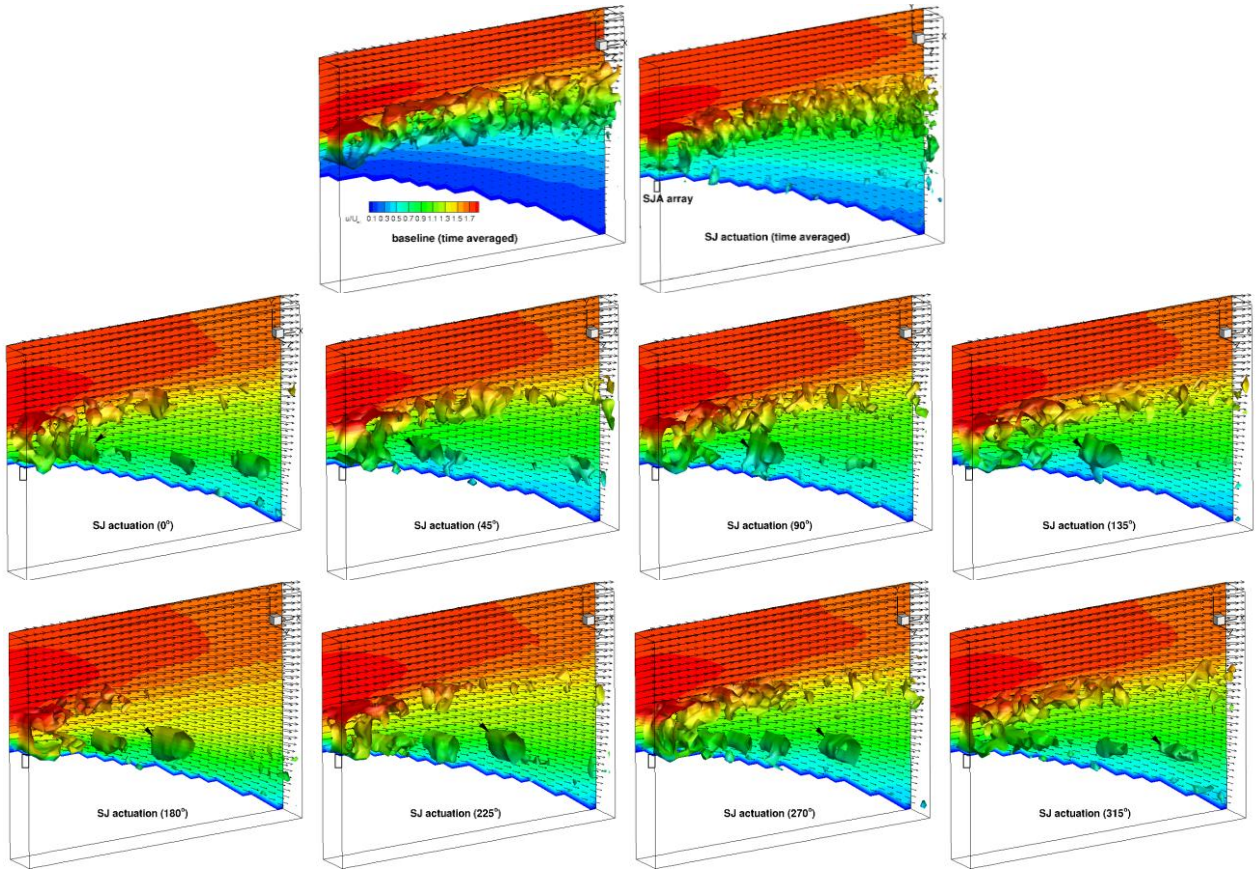

Fig. 2 Iso-surfaces of vortex structures colored by streamwise velocity for the time-averaged baseline case, time-averaged SJ actuation case and eight phase-averaged SJ actuation cases.

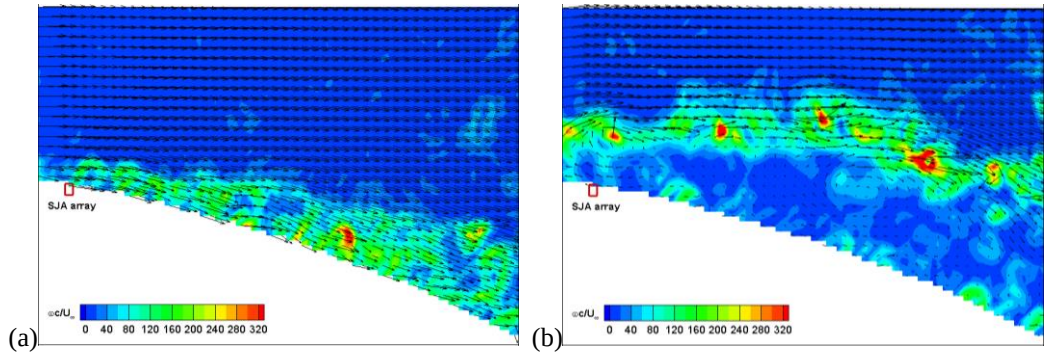

(a) (b)

Fig. 3 Instantaneous vorticity contours superimposed on velocity vectors in the *x*-*y* plane right across the center of a SJ actuator, showing (a) attached flow and (b) separated flow.

velocity field, and M the total number of snapshots used in the calculation.

Figure 4 shows the cumulative distribution of eigen energy, $E_n = \lambda_n/\Sigma\lambda_n$, for the first 200 POD modes of the baseline case and the case of SJ actuation at 0° phase angle. It can be observed that, for both the baseline and SJ actuation cases, the energy contribution by the first mode is significant, whereas, the remaining modes have marginal energy contribution. This indicates that the energy carried by the first mode's large-scale structures dominates the fluctuation of the flow field in both cases.

The vortex structures for the first POD mode are presented in Fig. 5 for both the baseline and SJ-actuation cases. Both cases share a very similar first mode, i.e., a 2D plane jet-like flow over the wing surface. Depending on the sign of its temporal coefficient, q_1, this mode represents either a momentum-injection flow (positive q_1) or an inverse flow (negative q_1) on top of the mean flow. As a result, positive q_1 values correspond to snapshots with an attached flow, whereas

negative q_1 values correspond to snapshots with a separated flow. Although introduction of the SJ array seems to have little effects on the first POD mode, it significantly increases the occurrence rate of positive q_1 values, or in another word, the possibility of flow attachment. In the present study, the ratio of the number of positive q_1 values to the total number of snapshots is about 30% for the baseline case and 65% for the SJ-actuation case. This proves the capability of the present SJ array in influencing the stability of the separated shear flow so as to increase the occurrence rate of flow re-attachment.

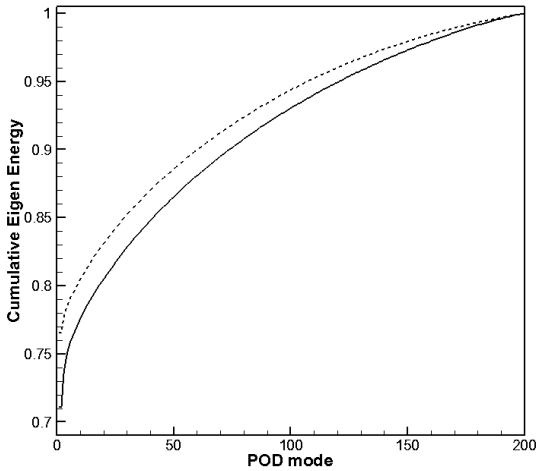

Fig. 4: Cumulative distribution of eigen energy for the baseline case (continuous line) and the phase averaged SJ actuation case (dashed line).

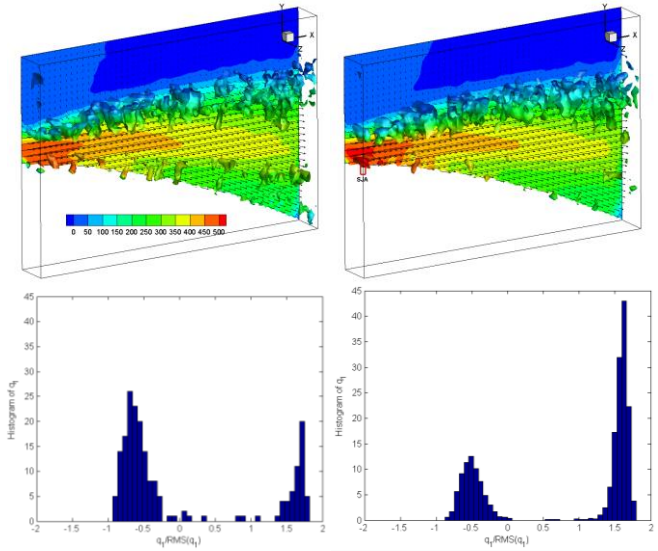

Fig. 5 Upper row: iso-surfaces of vortex structures for the first POD mode of (left) the baseline case and (right) the SJ actuation case. Lower row: distribution of q_1 values for (left) the baseline case and (right) SJ actuation case.

CONCLUSIONS

This paper unravels the flow-field over the suction surface of a LS(1)-0421 wing model using Tomo-PIV measurements. The PIV results showed that, after the SJ actuation large-size vortex structures in the shear layer were broken into small discrete structures. The reduction in the shear layer strength, the increase in near-wall flow velocity and the shift of shear layer trajectory towards the wing surface were found to be the impacts of the mild SJ control. Subsequently, POD analysis was carried out to extract the energetic flow structures from the flow field. It was observed that for the baseline case and different phase-averaged SJ actuation cases, the first mode is the dominant mode in the flow field that carries significant amount of energy. Although it seems that the present SJ array is not strong enough to change the first and dominant POD mode, the analysis of the coefficients of the first mode for all flow field snapshots reveals that the introduction of the SJ array significantly increases the possibility of flow attachment.

ACKNOWLEDGMENT

The authors of this paper are grateful for the financial support from Ministry of Education, Singapore, through Academic Research Fund (AcRF) Tier 1.

REFERENCES

[1] Smith BL, Glezer A, 1998, "The formation and evolution of synthetic jets," *Phys. Fluids* 10(9):2281.

[2] Amitay M, Smith DR, Kibens V, Parekh DE, Glezer A. 2001, "Aerodynamic flow control over an unconventional airfoil using synthetic jet actuators," *AIAA J.* 39(3):361–370.

[3] Amitay M, Glezer A, 2002, "Role of actuation frequency in controlled flow reattachment over a stalled airfoil," *AIAA J.* 40(2):209–216.

[4] Zhong S, Jabbal M, Tang H, Garcillan L, Guo F, Wood N, Warsop C, 2007, "Towards the design of synthetic-jet actuators for full-scale flight conditions," *Flow Turbul. Combust.* 78(3-4):283–307.

[5] Zhong S, Zhang S, 2013, "Further examination of the mechanism of round synthetic jets in delaying turbulent flow separation," *Flow Turbul. Combust.* 91(1): 177–208.

[6] Tang H, Salunkhe P, Zheng Y, Du J, Wu, Y, 2014 "On the use of synthetic jet actuator arrays for active flow separation control," *Exp. Therm. Fluid Sci.* 57:1–10

[7] Mccormick D, 2000, "Boundary layer separation control with directed synthetic jets," AIAA Paper 2000–0519.

[8] Crook A, Wood N, 2001, "Measurements and visualisations of synthetic jets," AIAA Paper 2001–0145.

[9] Melton L, Yao C, Seifert A, 2004, "Application of excitation from multiple locations on a simplified high-lift system," AIAA Paper 2004–2324.

[10] Ciuryla M, Liu Y, Farnsworth J, Kwan C, Amitay M, 2007, "Flight control using synthetic jets on a cessna 182 model," *J. Aircraft* 44:642–653.